SNS 110040300-DA0001-R00

Detailed SNS Neutronics Calculations for Scattering Instrument Design: SCT Configuration

July 2002

Detailed SNS Neutronics Calculations for Scattering Instrument Design: SCT Configuration
SNS 110040300-DA0001-R00

E. B. Iverson P. D. Ferguson F. X. Gallmeier I. I. Popova

Date Published: July 2002

Prepared for the
U.S. Department of Energy
Office of Science

UT-BATTELLE, LLC
managing
Spallation Neutron Source activities at

Argonne National Laboratory	Brookhaven National Laboratory
Thomas Jefferson National Accelerator Facility	Lawrence Berkeley National Laboratory
Los Alamos National Laboratory	Oak Ridge National Laboratory

under contract DE-AC05-00OR22725
for the
U.S. DEPARTMENT OF ENERGY

This document describes the neutronic performance characteristics predicted for a particular configuration of moderators in the Spallation Neutron Source High Power Target Station (SNS-HPTS). The configuration described herein is denoted “SCT.”

1 Model Description

Configuration SCT includes four moderators, two of which are viewed from both sides. All moderators have nominal viewed faces of 100 mm (horizontal) by 120 mm (vertical). The inner reflector (out to a radius of ≈320 mm) is beryllium and is cooled with heavy water. This inner reflector is surrounded by heavy water-cooled stainless steel. Table 1 summarizes relevant characteristics of the target station configuration used for this set of calculations. Although the SNS is designed for 2 MW operation as shown in Table 1, the initial construction will provide 1.44 MW operation. As our past calculations are normalized for 2 MW operation, we present these calculations with that same normalization.

Proton Energy	1 GeV
Pulse Rate	60 Hz
Average Power	2 MW
Energy per pulse	34 kJ
Proton Beam Shape	rectangular
Proton Beam Size	200x70 mm^2
Proton Pulse	$\delta(t)$
Target	Hg
Inner Reflector	Be
I.R. Coolant	D_2O
Outer Reflector	SS
O.R. Coolant	D_2O

Table 1: Target station parameters used in calculations. All normalizations are performed per 34 kJ-pulse.

Table 2 summarizes and Figure 1 illustrates the moderator configuration. The top upstream moderator is cadmium-decoupled hydrogen (assumed to be 100% parahydrogen) at 20 K and has curved viewed surfaces. The moderator material has a maximum thickness of 60 mm, and an average thickness of about 55 mm. The moderator is poisoned at the centerline with gadolinium 0.8 mm thick and is viewed from both sides. The top downstream

Beamline	Moderator Location	Moderator Material	T (K)	Decoupling Material	Poison Material	Poison Depth (mm)
2	TU	H_2	20	Cd	Gd	29.6
11	TU	H_2	20	Cd	Gd	29.6
5	TD	H_2	20	–	–	–
14	BD	H_2	20	–	–	–
8	BU	H_2O	300	Cd	Gd	14.75
17	BU	H_2O	300	Cd	Gd	24.75

Table 2: Moderator summary. H_2 is 20 K supercritical, modeled as liquid parahydrogen at supercritical density.

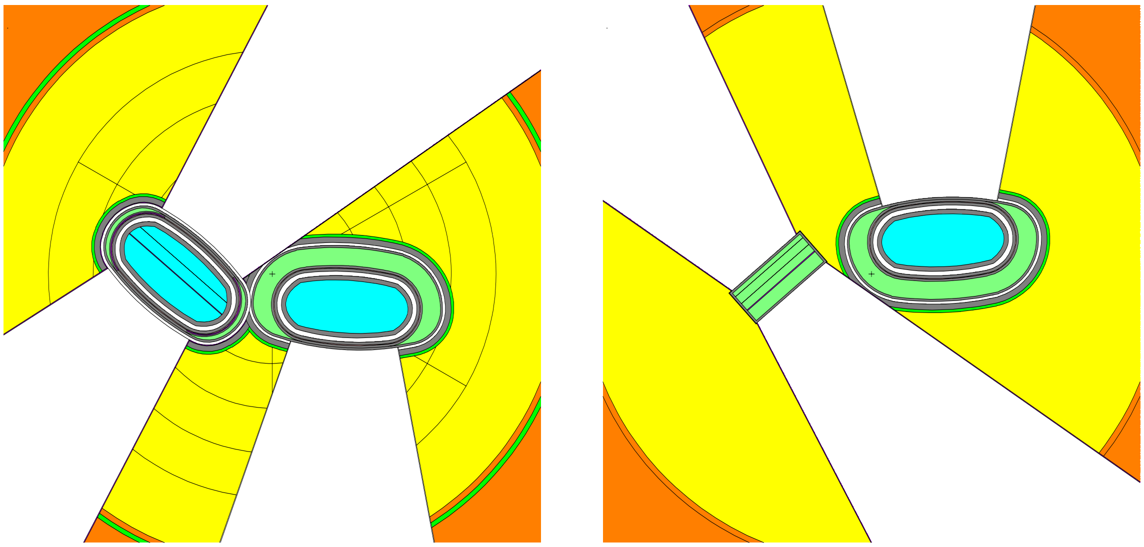

(a) Top Moderators (b) Bottom Moderators

Figure 1: SNS moderator configuration. Elevations shown are the centers of the upstream moderators. Protons enter from the left. Beamlines are numbered counterclockwise beginning at the proton beam.

moderator is fully coupled unpoisoned hydrogen (again parahydrogen) at 20 K, and is viewed from one side only. This moderator also has a curved viewed surface, with maximum thickness of 60 mm, and an average thickness of about 55 mm. This moderator also has approximately 20 mm of light water surrounding it as premoderator. The bottom downstream moderator is identical to the top downstream moderator. The bottom upstream moderator is cadmium-decoupled water at 300 K with flat viewed surfaces. The moderator material is 40.5 mm thick, and is assymetrically poisoned with gadolinium 1 mm thick. This moderator is viewed from both sides.

2 Calculational Techniques

The simulations reported are the results of calculations using the MCNPX code from LANL (version 2.1.5). [1] The spectral intensities shown result from calculations using point detector tallies located 10 m from the viewed surface of the moderator. Artificial collimating masks between the point detector locations and the moderator surfaces limit the tallied view of the moderator to a 100 mm horizontal by 120 mm vertical view of the moderator, centered on the viewed face. The emission time distributions (pulse shapes) come from current tallies on the viewed surface of the moderator material, and are averaged over 2π steradians. Weight windows to accelerate the pulse shape calculations were generated by separate iterative runs using MCNPX in parallel mode on a large cluster of machines with a neutron-only source term. MCNPX runs using these weight windows produced the reported results, which have further been scaled (from the point detector calculations) to correspond to the peak intensity coming off of the moderator face in the normal direction, rather than the average over 2π steradians. Each moderator requires a unique set of weight windows, and thus a unique set of runs.

3 Extrapolation

The results of the various simulations are reported, both here and in the source files (see also Section 6), over a broad range of energies. If predictions for energies outside this range are desired, certain extrapolations are reasonable. Spectra can be extrapolated to these higher energies by using a simple power law, as they are nearly $1/E$ up to energies of approximately 100 keV. Emission time distributions at higher energies can in general be assumed to be invariant as a function of vt (velocity multiplied by time), equivalent to t/λ. However, the proton pulse at SNS is not actually a delta function in time, but rather has a width of a few hundred nanoseconds, and is shown in Figure 2. [2] Neutron pulse shapes for energies above 10 eV or so will be influenced by this proton pulse shape, while neutron

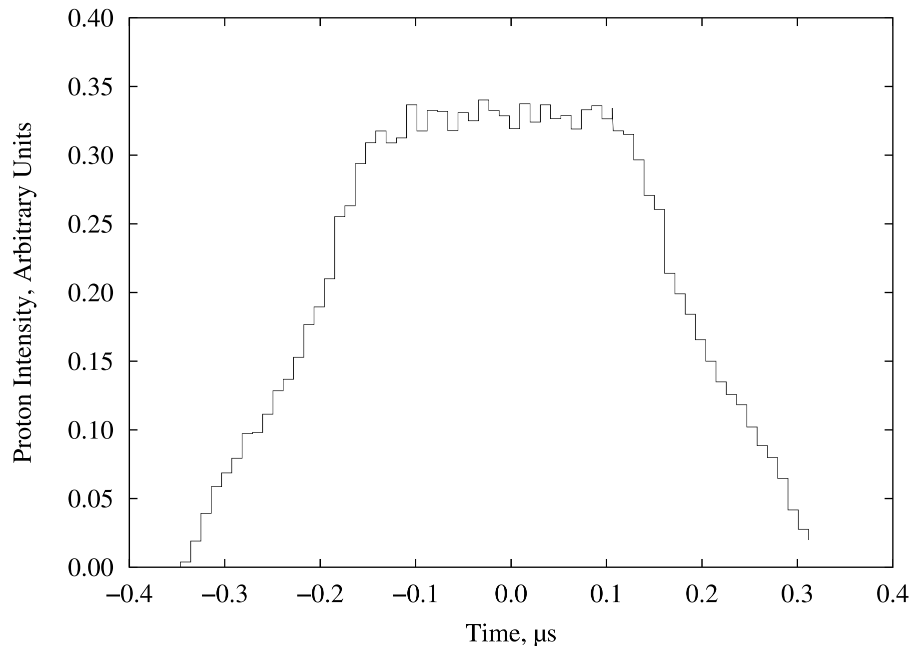

Figure 2: Time distribution of protons arriving at SNS Target.

pulse shapes for energies above 300 eV or so will be completely dominated by the proton pulse shape, and thus will be invariant as a function of time.

At low energies, the spectral intensity from all of the moderators can again be assumed to obey a power law distribution. The low-energy intensity from the moderators will not correspond to a Maxwellian distribution in the case of either water or hydrogen. The pulse shapes at low energies are approximately invariant in time for water and for coupled hydrogen, and approximately invariant in vt for decoupled parahydrogen.

4 Metrics

Various “metrics” characterizing the spectra and pulse shapes are sometimes more useful than the fully detailed source. We have calculated the following metrics for each neutron beam: total intensity, peak intensity, peak time, full-width at half-maximum, mean emission time, and root-mean-square emission time. Examples of these metrics appear in Figure 3.

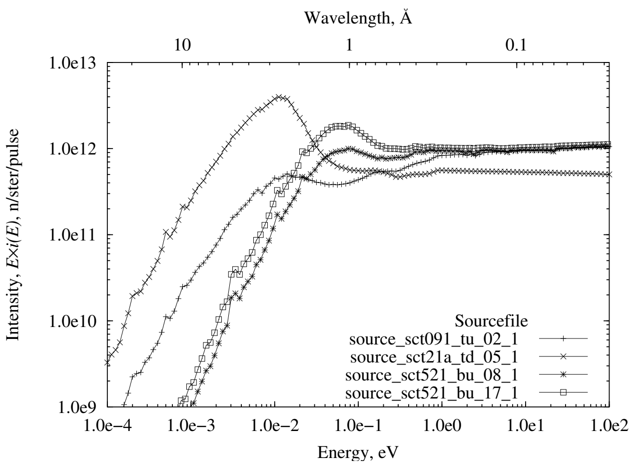

(a) Intensity per unit lethargy

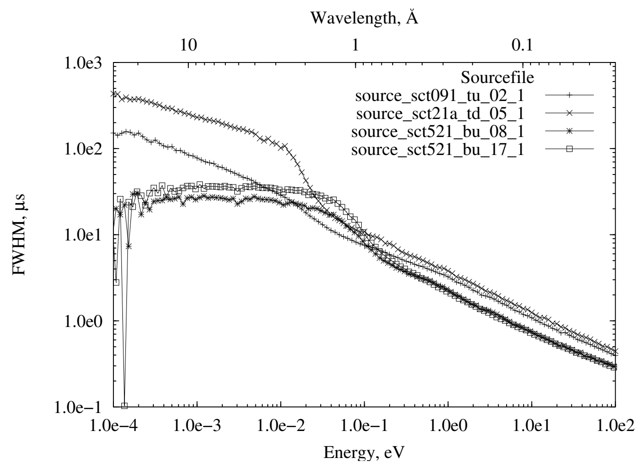

(b) Full-Width at Half-Maximum

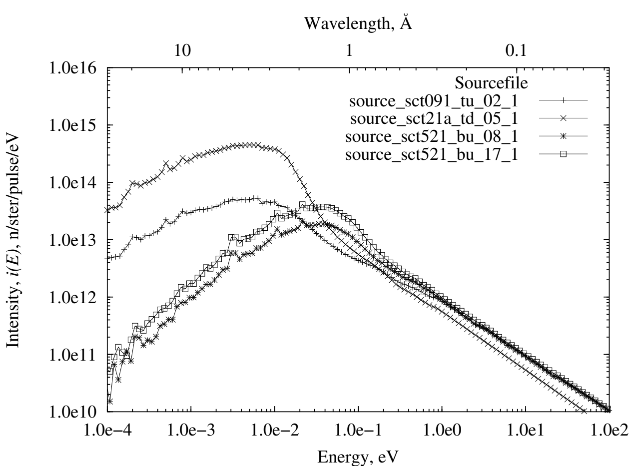

(c) Intensity per unit energy

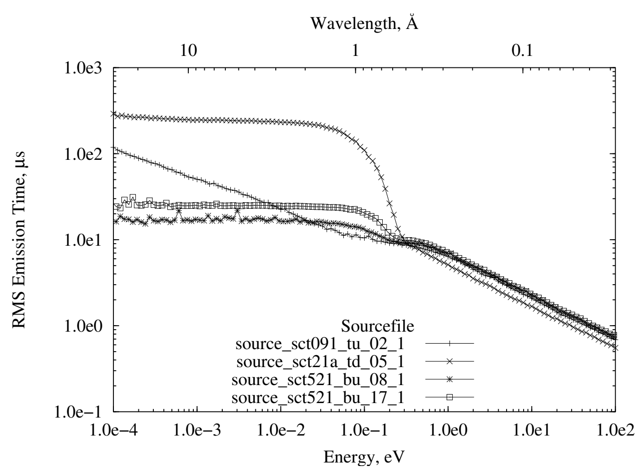

(d) RMS emission time

Figure 3: Selected metrics for all moderators.

5 Parametric Descriptions

The calculated spectra can be described moderately well by analytical forms. The function

$$i(E) = I_{\text{epi}} e^{-c/\sqrt{E}} \left(R \frac{E}{(kT)^2} e^{-E/kT} + \Delta(E) \frac{1}{E^{1-\alpha}} \right), \tag{1}$$

combines a slowing-down spectrum and a Maxwellian using a generalized Westcott joining function $\Delta(E)$,

$$\Delta(E) = \frac{1}{1 + (E_{\text{co}}/E)^s}. \tag{2}$$

Equation 1 provides a good description of the energy spectra from the SNS water moderators as shown in Figure 4. Discrepancies appear near 1–3 eV (as the slowing-down term does not allow for flux depressions near resonances

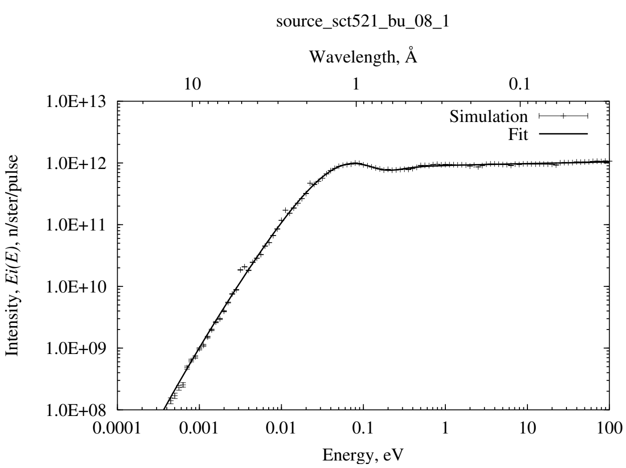

(a) High-Resolution Water

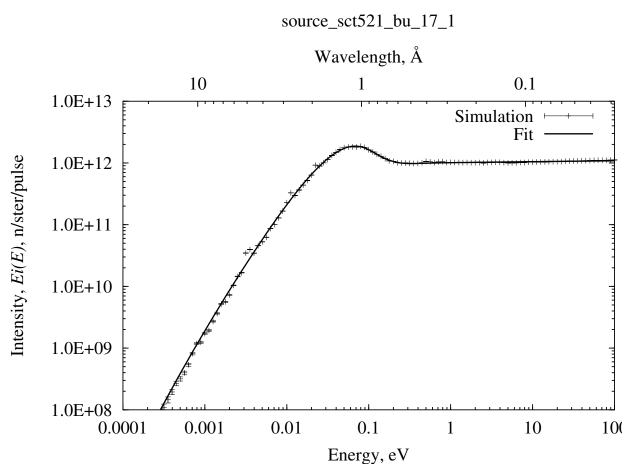

(b) High-Intensity Water

Figure 4: Parametric fits to the spectral intensities from water moderators.

in the gadolinium poison [3]) and at various energies from 3–30 meV (due to discretization artifacts in the $S(\alpha, \beta)$ treatment in MCNPX [4]). The energy-dependent factor $e^{-c/\sqrt{E}}$ mimics the action of a $1/v$ absorber, although it does not correspond to attenuation due to material in the beamline. (If this term were to be interpreted as absorption due to material in the neutron beamline—for example, the aluminum alloy forming the moderator vessel—it would imply approximately 1 m of aluminum in the beamline, which is obviously not the case.) We attribute this behavior to a diffusion heating-like effect in the moderator material.

Brun [5] suggests a function

$$\rho(E) = 1 + \delta_\rho e^{-x} \left(1 + x + \frac{1}{2} x^2 \right), \tag{3}$$

where

$$x(E) = \begin{cases} \gamma(E - 2B) & E > 2B \\ 0 & E \leq 2B, \end{cases} \tag{4}$$

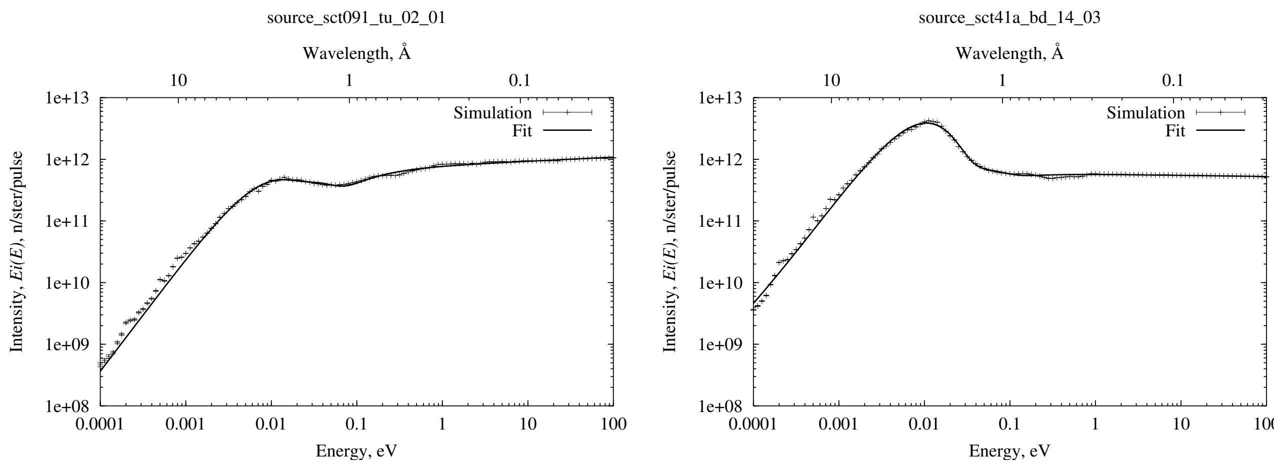

(a) Decoupled Poisoned Hydrogen (b) Coupled Hydrogen

Figure 5: Parametric fits to the spectral intensities from hydrogen moderators.

B is the free hydrogen rotational constant (7.36 meV), and δ_ρ and γ are free parameters, "chosen to simulate the rapid change in the para-hydrogen cross section at $2B$." We incorporate this function ρ,

$$i(E) = I_{\text{epi}} e^{-c/\sqrt{E}} \left(R \frac{E}{(kT)^2} e^{-E/kT} + \Delta(E)\rho(E)\frac{1}{E^{1-\alpha}} \right) \tag{5}$$

to fit the spectra from the hydrogen moderators. Some of these fits are shown in Figure 5.

Parameters resulting from such fits are shown in Table 3. Although these parameterizations are inspired by a physics analysis of neutron slowing-down and thermalization, they do not model the simulated data well enough to have unique physical interpretations, and should be considered arbitrary "smoothing" functions. Although the general agreement appears good, χ^2_ν is high, typically around 400-2100. As mentioned above, the quality of the fits shown in Figures 4 and 5 is only moderate, but can certainly be trusted to better than 10% over the energy range 0.001–10 eV.

Beam	Moderator	I_{epi}	kT	R	c	E_{co}	s	α	δ_ρ	γ
		n/ster/eV/pulse	meV	-	$\sqrt{\text{eV}}$	meV	-	-	-	eV^{-1}
2TU	dec. pois. H_2	8.0×10^{11}	5.0	0.77	0.005	72.	1.23	0.066	1.70	103.
11TU	dec. pois. H_2	8.0×10^{11}	5.0	0.78	0.005	72.	1.23	0.066	1.72	99.
5TD	coupled H_2	5.5×10^{11}	5.1	11.2	0.000	23.	1.16	-0.017	0.72	52.
14BD	coupled H_2	5.7×10^{11}	5.1	11.5	0.000	23.	1.16	-0.019	0.74	51.
8BU	dec. pois. H_2O	9.3×10^{11}	32.	1.9	0.016	135.	2.82	0.025	-	-
17BU	dec. pois. H_2O	10.3×10^{11}	33.	3.6	0.017	155.	4.89	0.012	-	-

Table 3: Spectral parameterizations of moderator performances.

6 Data Availability

These results are available electronically as "source files;" ASCII files containing the spectra and emission time distributions, with comments showing the file format. Each moderator is represented by a single source file. These source files can be downloaded from http://www.sns.anl.gov under "Components/Moderators," or obtained from the author. The metrics described above are similarly available. Beamlines are associated with source and metrics files as given in Table 4.

Beam	Moderator	Source File	Metrics File
2TU	dec. pois. H_2	`source_sct091_tu_02_1.dat`	`source_sct091_tu_02_1_metrics.dat`
11TU	dec. pois. H_2	`source_sct091_tu_11_1.dat`	`source_sct091_tu_11_1_metrics.dat`
5TD	coupled H_2	`source_sct21a_td_05_1.dat`	`source_sct21a_td_05_1_metrics.dat`
14BD	coupled H_2	`source_sct41a_bd_14_1.dat`	`source_sct41a_bd_14_1_metrics.dat`
8BU	dec. pois. H_2O	`source_sct521_bu_08_1.dat`	`source_sct521_bu_08_1_metrics.dat`
17BU	dec. pois. H_2O	`source_sct521_bu_17_1.dat`	`source_sct521_bu_17_1_metrics.dat`

Table 4: Source file and metrics file names.

7 Detailed Pulse Shapes

Some of the detailed emission time distributions (pulse shapes) as produced with the simulations appear below. The results for Beamlines 2 and 11 are nominally identical; only results for Beamline 2 are shown here. Similarly, results for Beamline 5 should be similar to those for Beamline 14.

References

[1] L. S. Waters, "MCNPX^{tm} user's manual," Tech. Rep. LA-UR 99-6058, Los Alamos National Laboratory, November 1999.

[2] J. D. Galambos, March 2002. Private Communication.

[3] E. B. Iverson and B. D. Murphy, "Burn-up of moderator poison in pulsed neutron sources," in *Proceedings of the 4th International Topical Meeting on Nuclear Applications of Accelerator Technology, AccApp'00*, pp. 109–115, American Nuclear Society, November 2000.

[4] R. E. MacFarlane, "Cold-moderator scattering kernel methods," in *Proceedings of the International Workshop on Cold Moderators for Pulsed Neutron Sources* (J. M. Carpenter and E. B. Iverson, eds.), pp. 221–231, OECD, 1998.

[5] T. O. Brun, "Spectra and pulse shapes of a decoupled liquid hydrogen moderator," in *Proceedings of the International Workshop on Cold Moderators for Pulsed Neutron Sources* (J. M. Carpenter and E. B. Iverson, eds.), pp. 163–170, OECD, 1998.

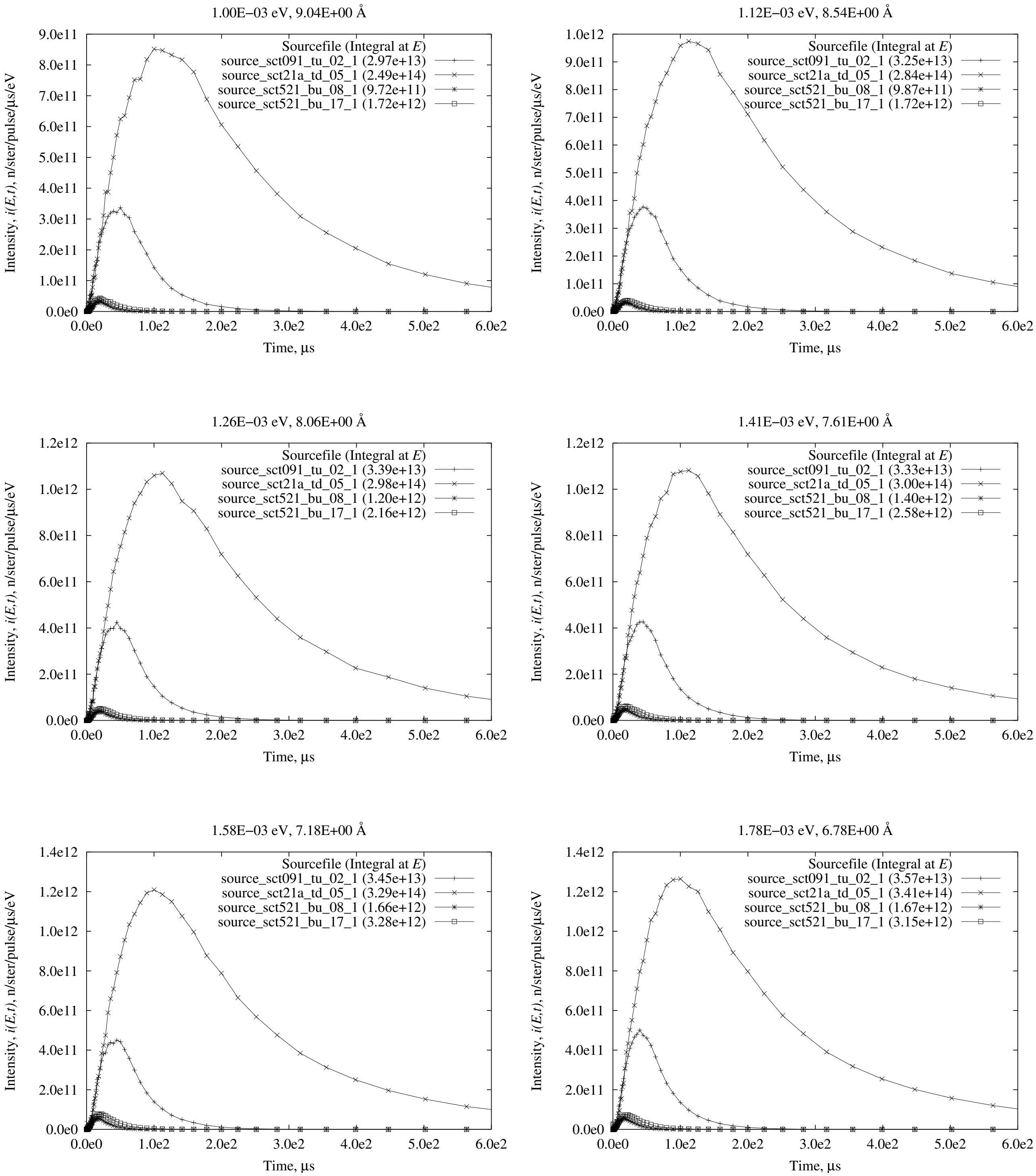

Figure 6: Emission time distributions. Results for 2TU (decoupled poisoned H_2) are denoted source_sct091_tu_02_1 and are similar to those for 11TU. Results for 5TD (coupled H_2) are denoted source_sct21a_td_05_1 and are similar to those for 14BD. Results for 8BU (decoupled H_2O poisoned at 15 mm) are denoted source_sct521_bu_08_1, and results for 17BU (decoupled H_2O poisoned at 25 mm) are denoted source_sct521_bu_17_1.

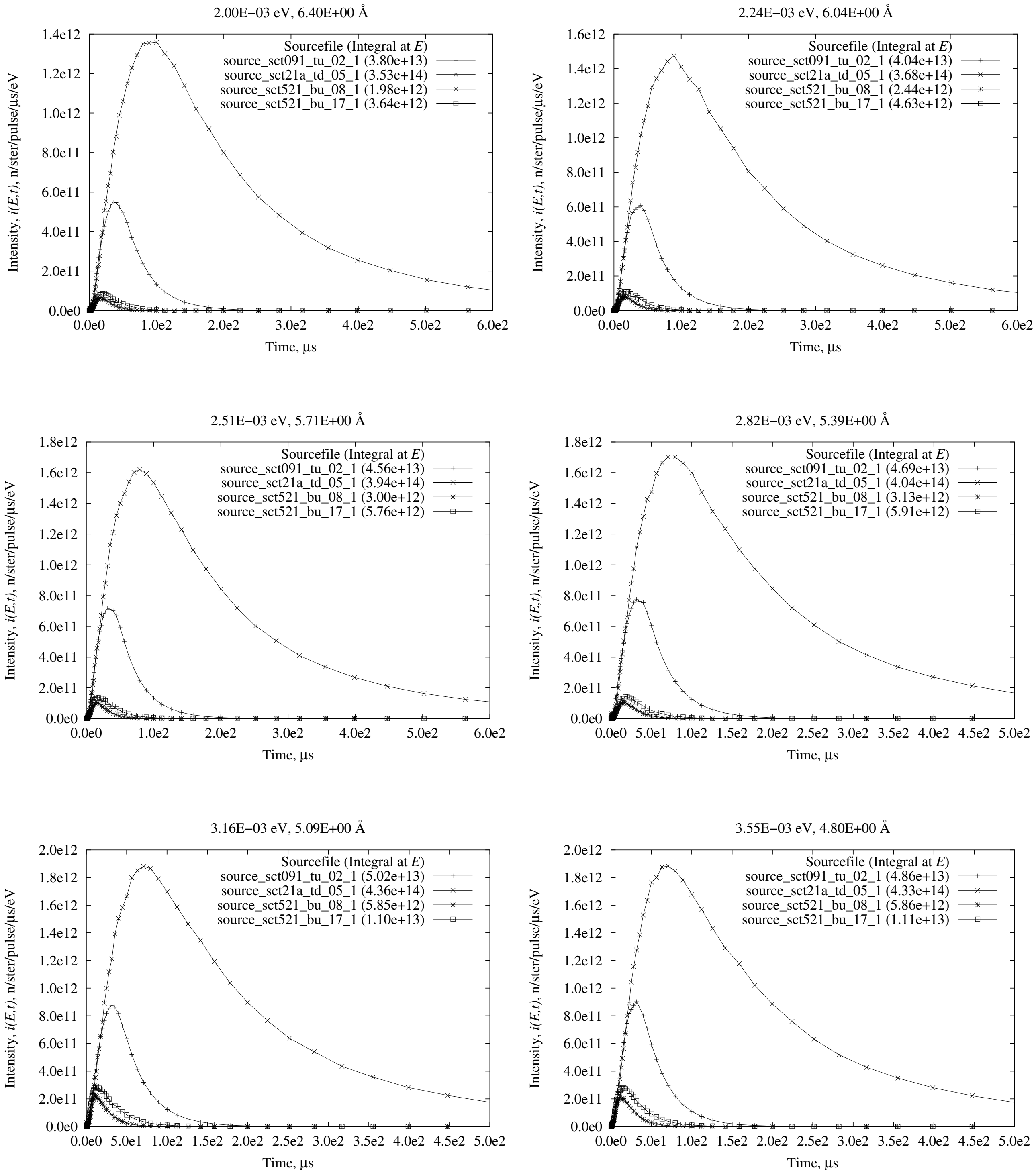

Figure 7: Emission time distributions. Results for 2TU (decoupled poisoned H_2) are denoted source_sct091_tu_02_1 and are similar to those for 11TU. Results for 5TD (coupled H_2) are denoted source_sct21a_td_05_1 and are similar to those for 14BD. Results for 8BU (decoupled H_2O poisoned at 15 mm) are denoted source_sct521_bu_08_1, and results for 17BU (decoupled H_2O poisoned at 25 mm) are denoted source_sct521_bu_17_1.

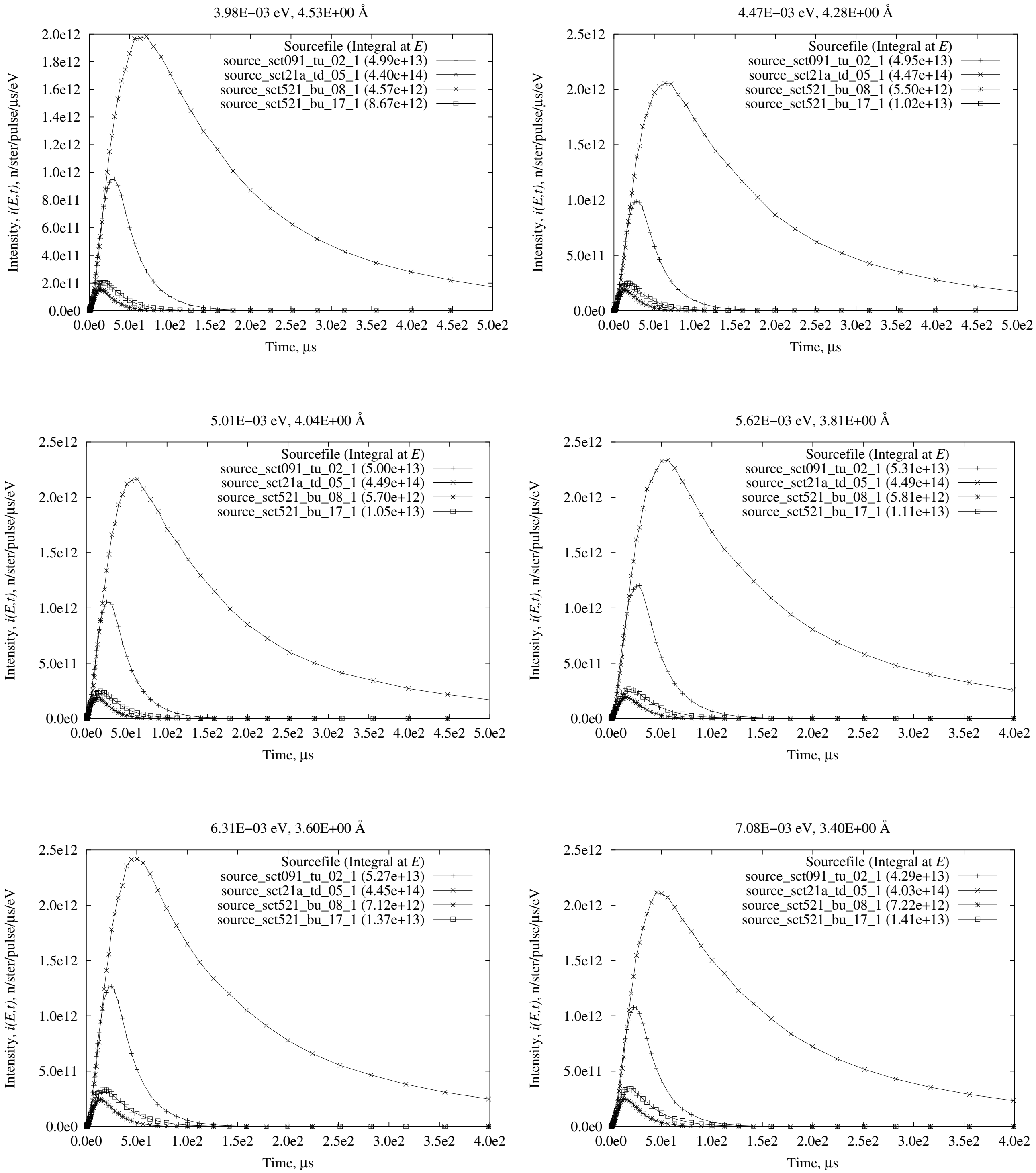

Figure 8: Emission time distributions. Results for 2TU (decoupled poisoned H_2) are denoted source_sct091_tu_02_1 and are similar to those for 11TU. Results for 5TD (coupled H_2) are denoted source_sct21a_td_05_1 and are similar to those for 14BD. Results for 8BU (decoupled H_2O poisoned at 15 mm) are denoted source_sct521_bu_08_1, and results for 17BU (decoupled H_2O poisoned at 25 mm) are denoted source_sct521_bu_17_1.

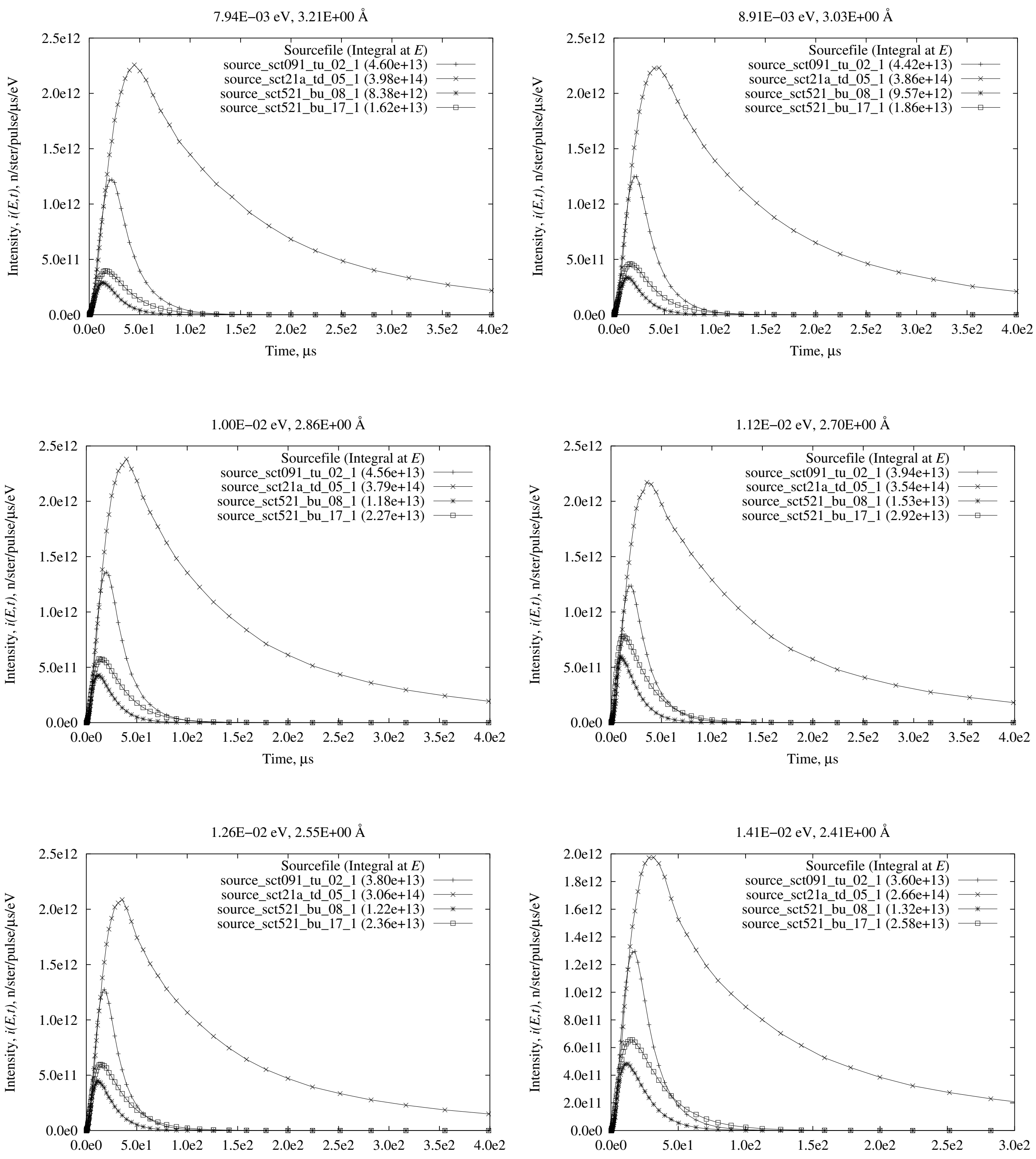

Figure 9: Emission time distributions. Results for 2TU (decoupled poisoned H_2) are denoted source_sct091_tu_02_1 and are similar to those for 11TU. Results for 5TD (coupled H_2) are denoted source_sct21a_td_05_1 and are similar to those for 14BD. Results for 8BU (decoupled H_2O poisoned at 15 mm) are denoted source_sct521_bu_08_1, and results for 17BU (decoupled H_2O poisoned at 25 mm) are denoted source_sct521_bu_17_1.

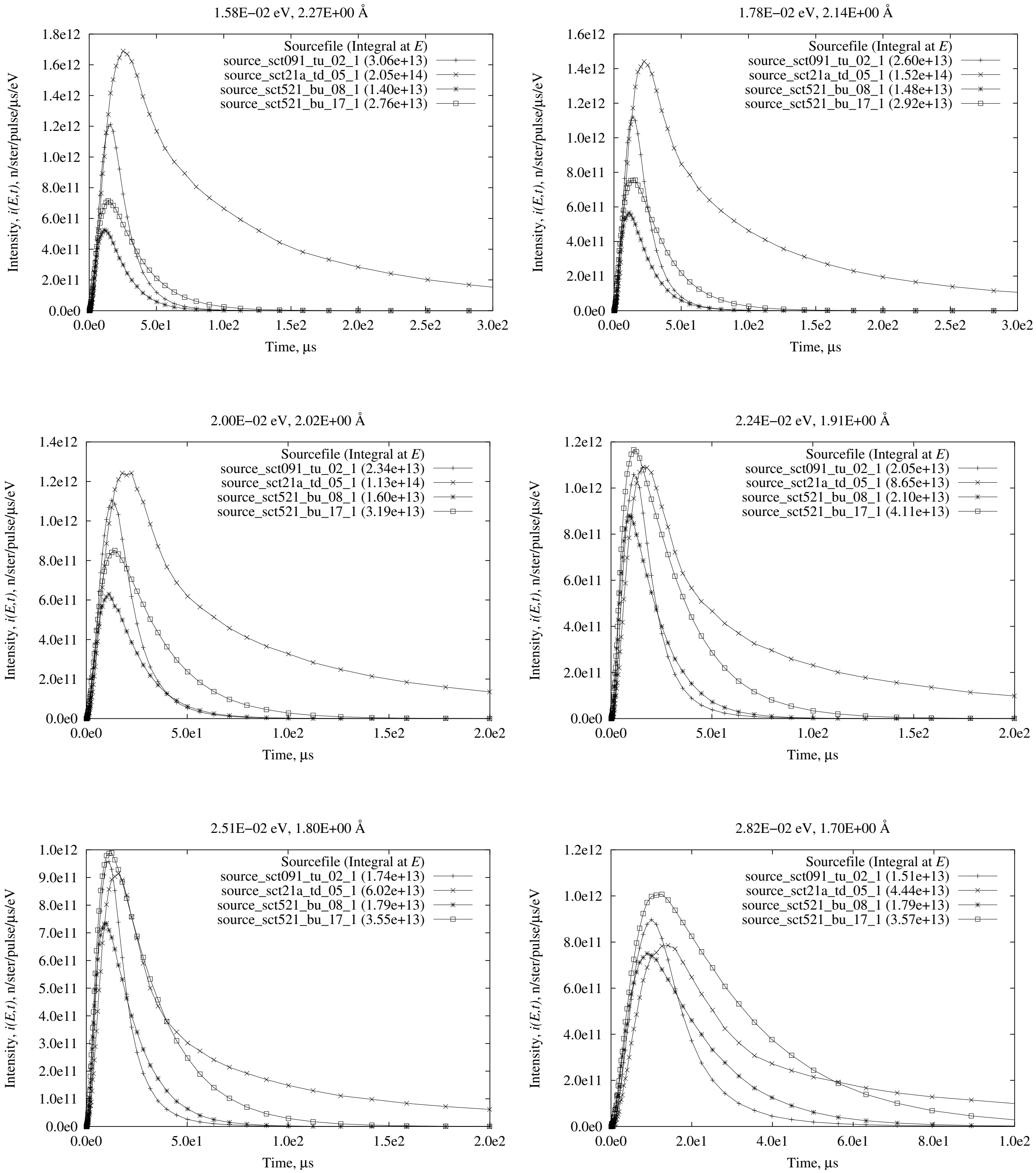

Figure 10: Emission time distributions. Results for 2TU (decoupled poisoned H_2) are denoted source_sct091_tu_02_1 and are similar to those for 11TU. Results for 5TD (coupled H_2) are denoted source_sct21a_td_05_1 and are similar to those for 14BD. Results for 8BU (decoupled H_2O poisoned at 15 mm) are denoted source_sct521_bu_08_1, and results for 17BU (decoupled H_2O poisoned at 25 mm) are denoted source_sct521_bu_17_1.

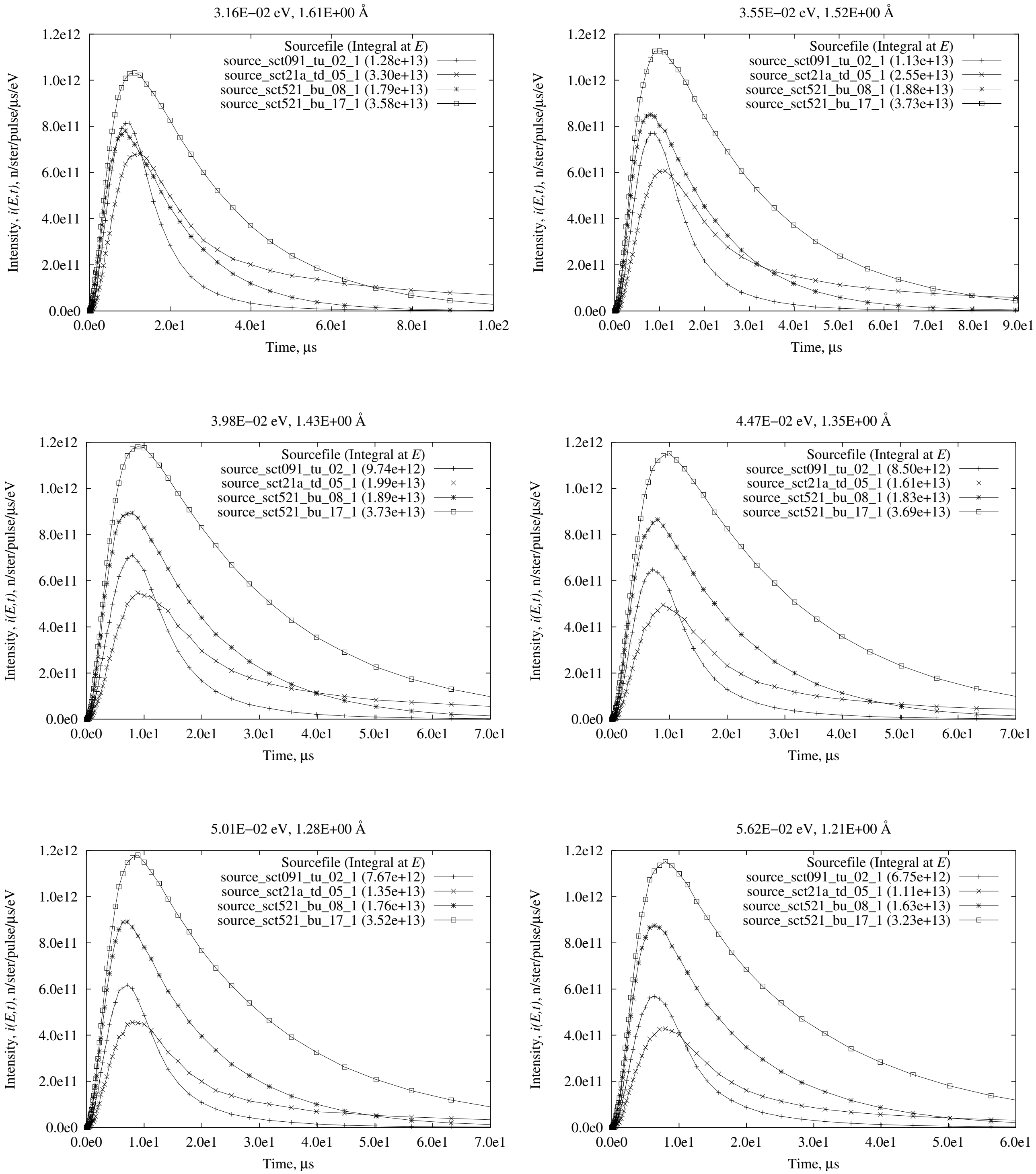

Figure 11: Emission time distributions. Results for 2TU (decoupled poisoned H_2) are denoted source_sct091_tu_02_1 and are similar to those for 11TU. Results for 5TD (coupled H_2) are denoted source_sct21a_td_05_1 and are similar to those for 14BD. Results for 8BU (decoupled H_2O poisoned at 15 mm) are denoted source_sct521_bu_08_1, and results for 17BU (decoupled H_2O poisoned at 25 mm) are denoted source_sct521_bu_17_1.

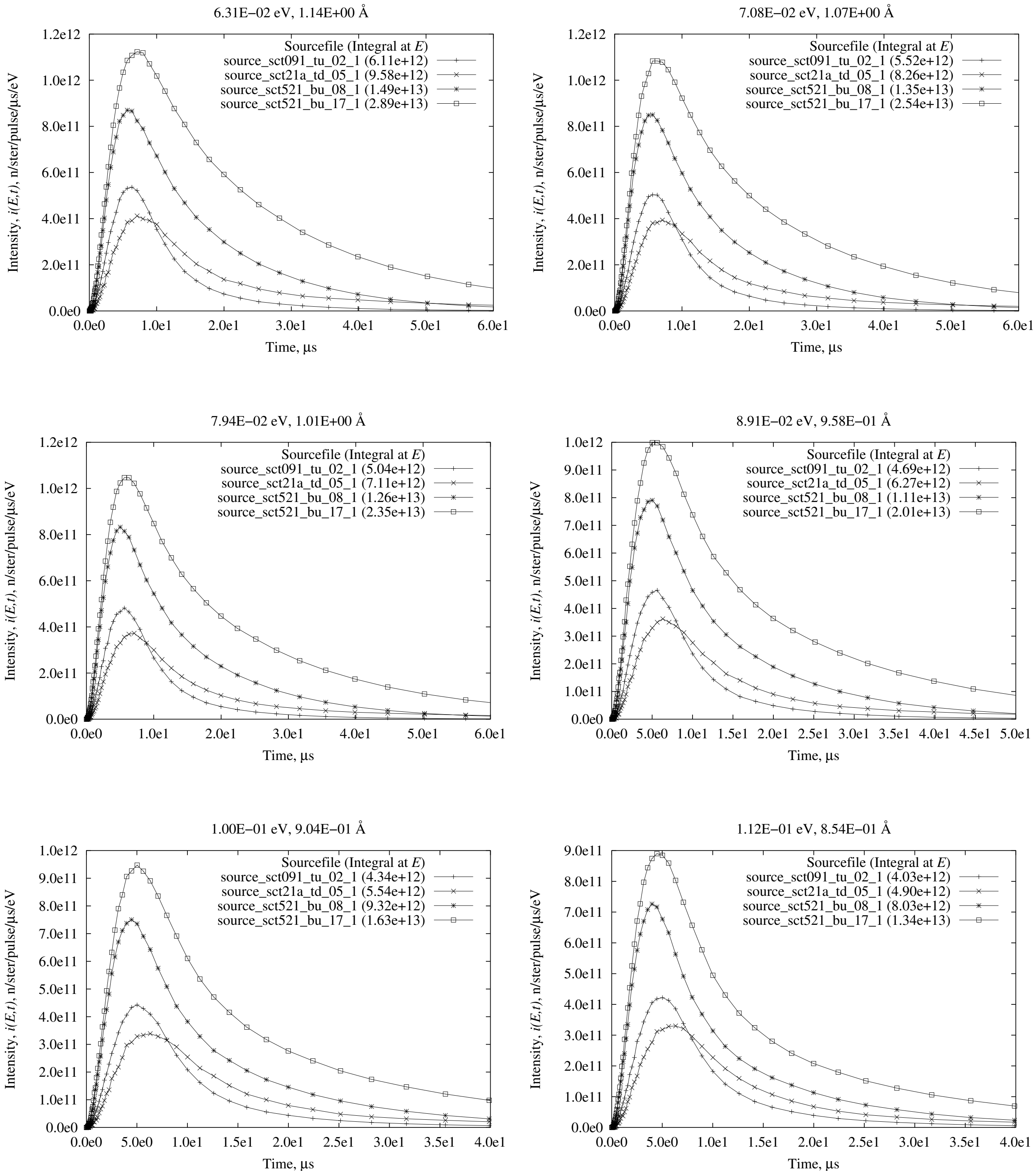

Figure 12: Emission time distributions. Results for 2TU (decoupled poisoned H_2) are denoted source_sct091_tu_02_1 and are similar to those for 11TU. Results for 5TD (coupled H_2) are denoted source_sct21a_td_05_1 and are similar to those for 14BD. Results for 8BU (decoupled H_2O poisoned at 15 mm) are denoted source_sct521_bu_08_1, and results for 17BU (decoupled H_2O poisoned at 25 mm) are denoted source_sct521_bu_17_1.

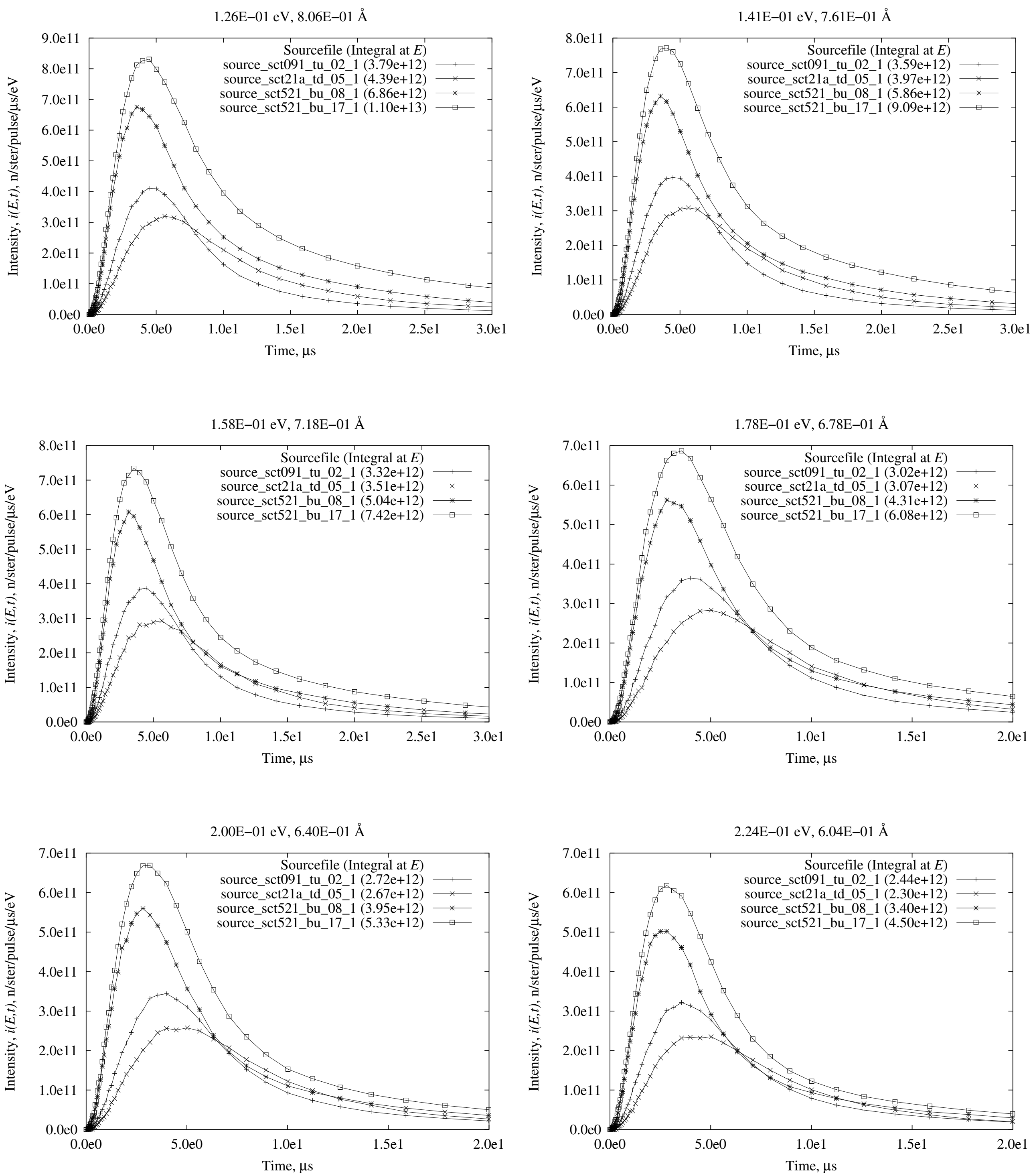

Figure 13: Emission time distributions. Results for 2TU (decoupled poisoned H_2) are denoted source_sct091_tu_02_1 and are similar to those for 11TU. Results for 5TD (coupled H_2) are denoted source_sct21a_td_05_1 and are similar to those for 14BD. Results for 8BU (decoupled H_2O poisoned at 15 mm) are denoted source_sct521_bu_08_1, and results for 17BU (decoupled H_2O poisoned at 25 mm) are denoted source_sct521_bu_17_1.

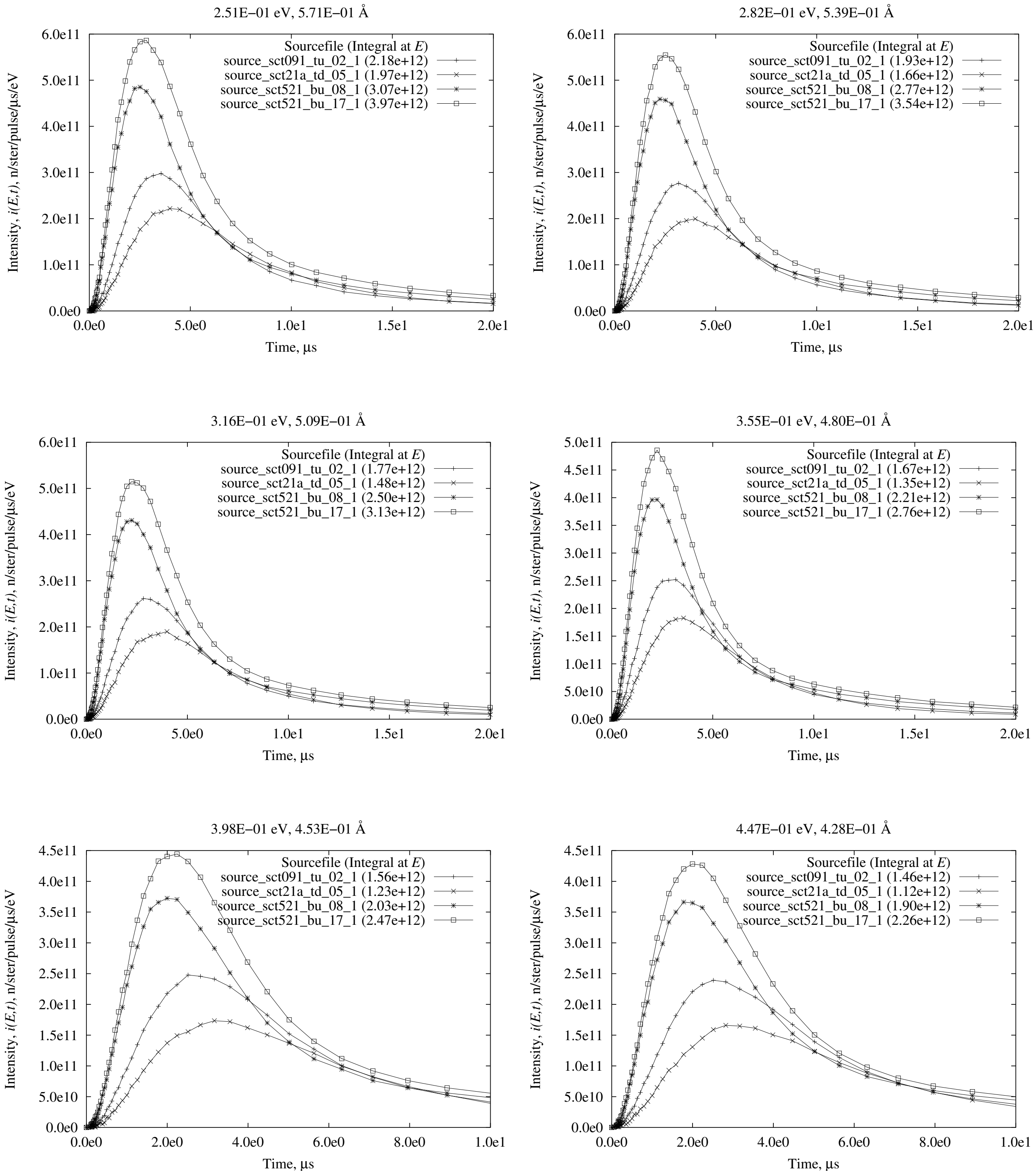

Figure 14: Emission time distributions. Results for 2TU (decoupled poisoned H_2) are denoted source_sct091_tu_02_1 and are similar to those for 11TU. Results for 5TD (coupled H_2) are denoted source_sct21a_td_05_1 and are similar to those for 14BD. Results for 8BU (decoupled H_2O poisoned at 15 mm) are denoted source_sct521_bu_08_1, and results for 17BU (decoupled H_2O poisoned at 25 mm) are denoted source_sct521_bu_17_1.

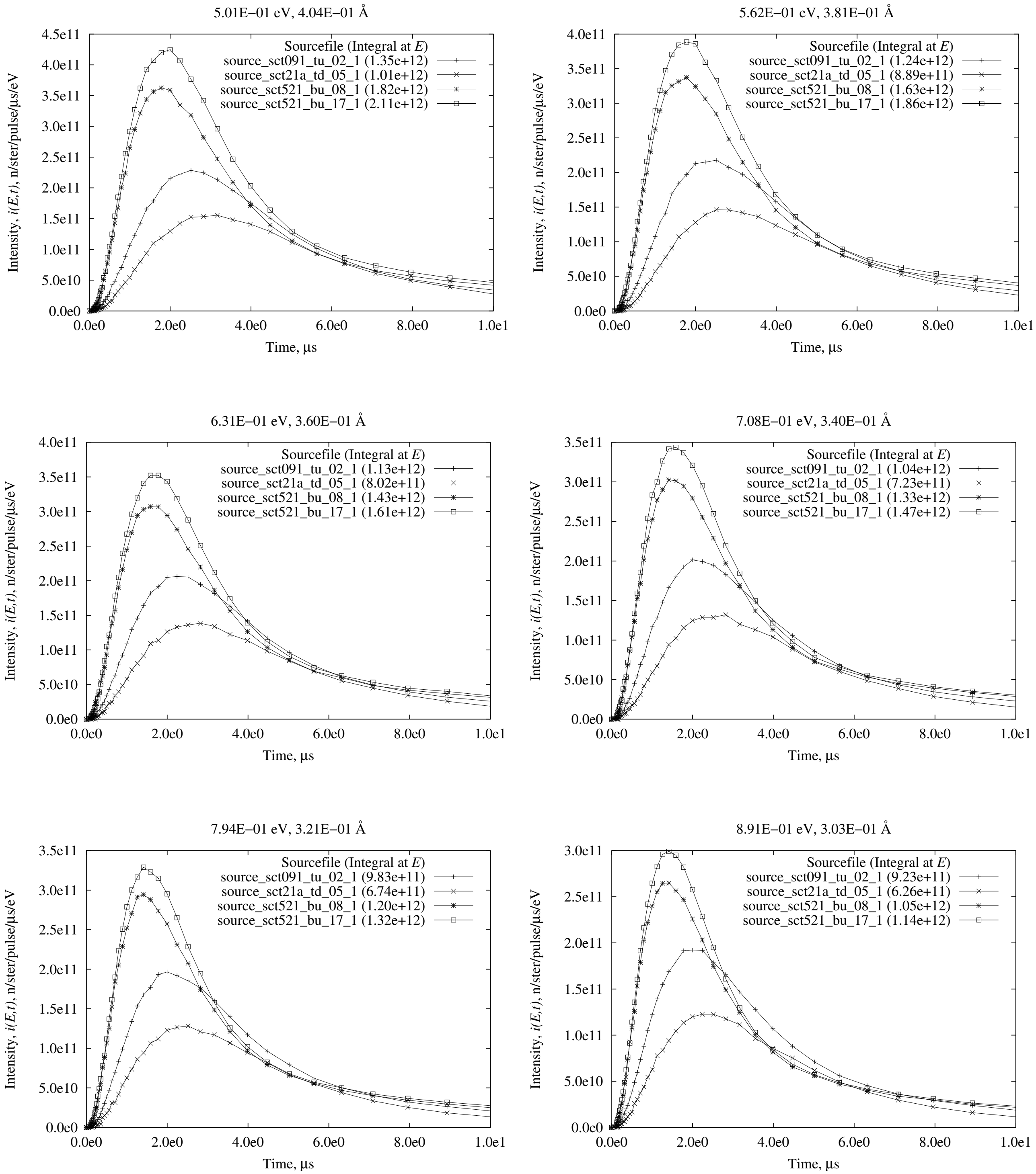

Figure 15: Emission time distributions. Results for 2TU (decoupled poisoned H_2) are denoted source_sct091_tu_02_1 and are similar to those for 11TU. Results for 5TD (coupled H_2) are denoted source_sct21a_td_05_1 and are similar to those for 14BD. Results for 8BU (decoupled H_2O poisoned at 15 mm) are denoted source_sct521_bu_08_1, and results for 17BU (decoupled H_2O poisoned at 25 mm) are denoted source_sct521_bu_17_1.

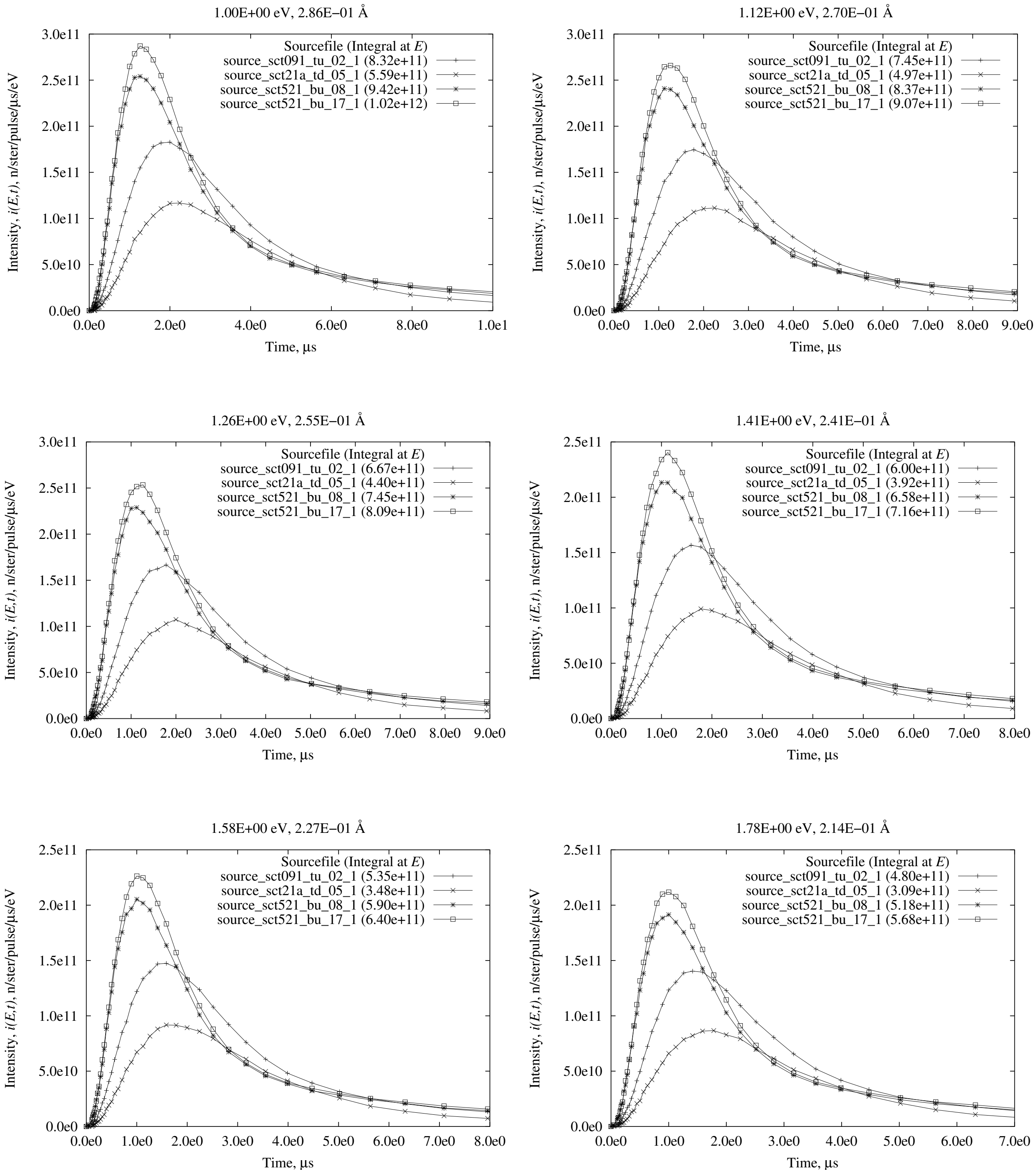

Figure 16: Emission time distributions. Results for 2TU (decoupled poisoned H_2) are denoted source_sct091_tu_02_1 and are similar to those for 11TU. Results for 5TD (coupled H_2) are denoted source_sct21a_td_05_1 and are similar to those for 14BD. Results for 8BU (decoupled H_2O poisoned at 15 mm) are denoted source_sct521_bu_08_1, and results for 17BU (decoupled H_2O poisoned at 25 mm) are denoted source_sct521_bu_17_1.

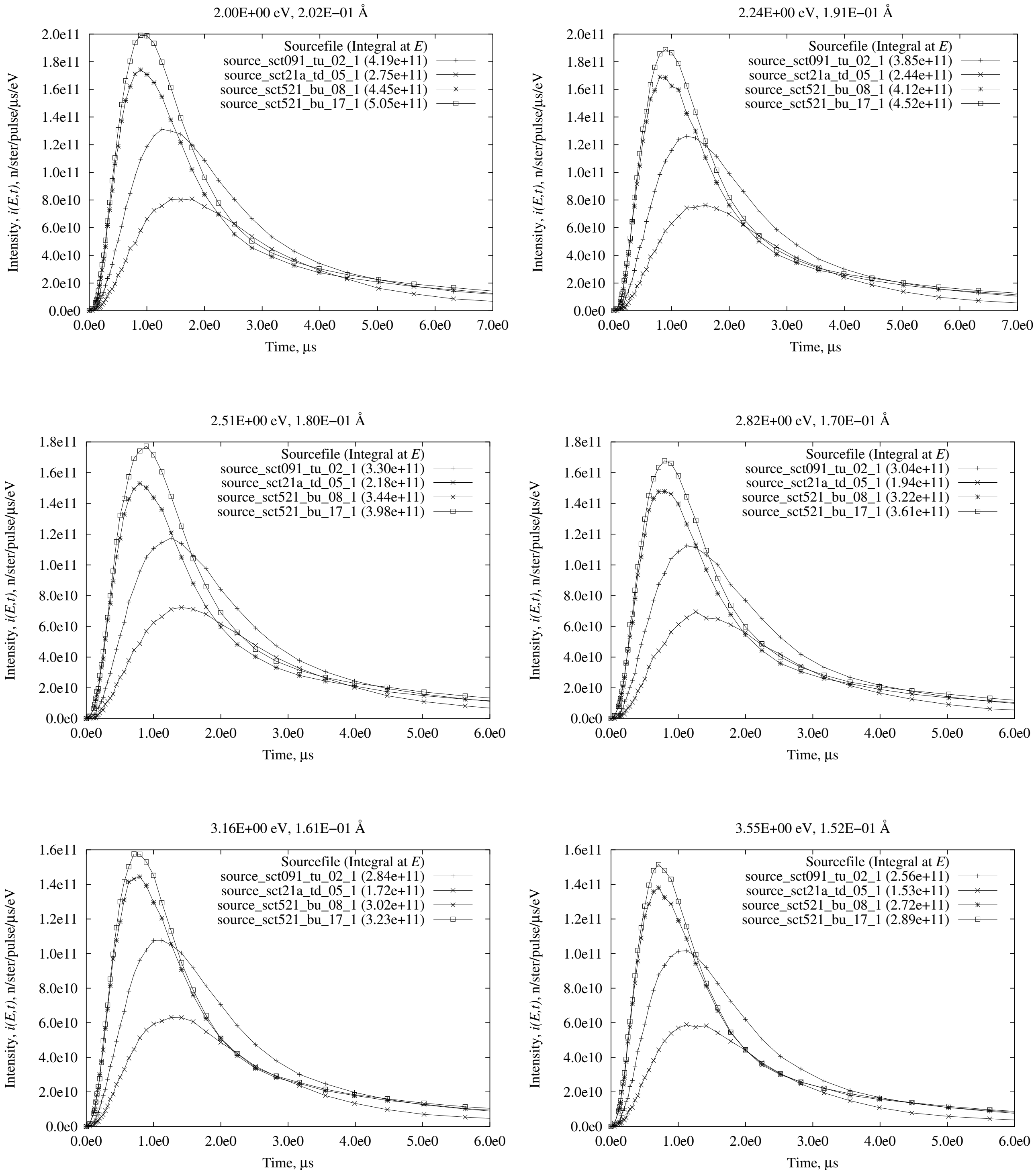

Figure 17: Emission time distributions. Results for 2TU (decoupled poisoned H_2) are denoted source_sct091_tu_02_1 and are similar to those for 11TU. Results for 5TD (coupled H_2) are denoted source_sct21a_td_05_1 and are similar to those for 14BD. Results for 8BU (decoupled H_2O poisoned at 15 mm) are denoted source_sct521_bu_08_1, and results for 17BU (decoupled H_2O poisoned at 25 mm) are denoted source_sct521_bu_17_1.

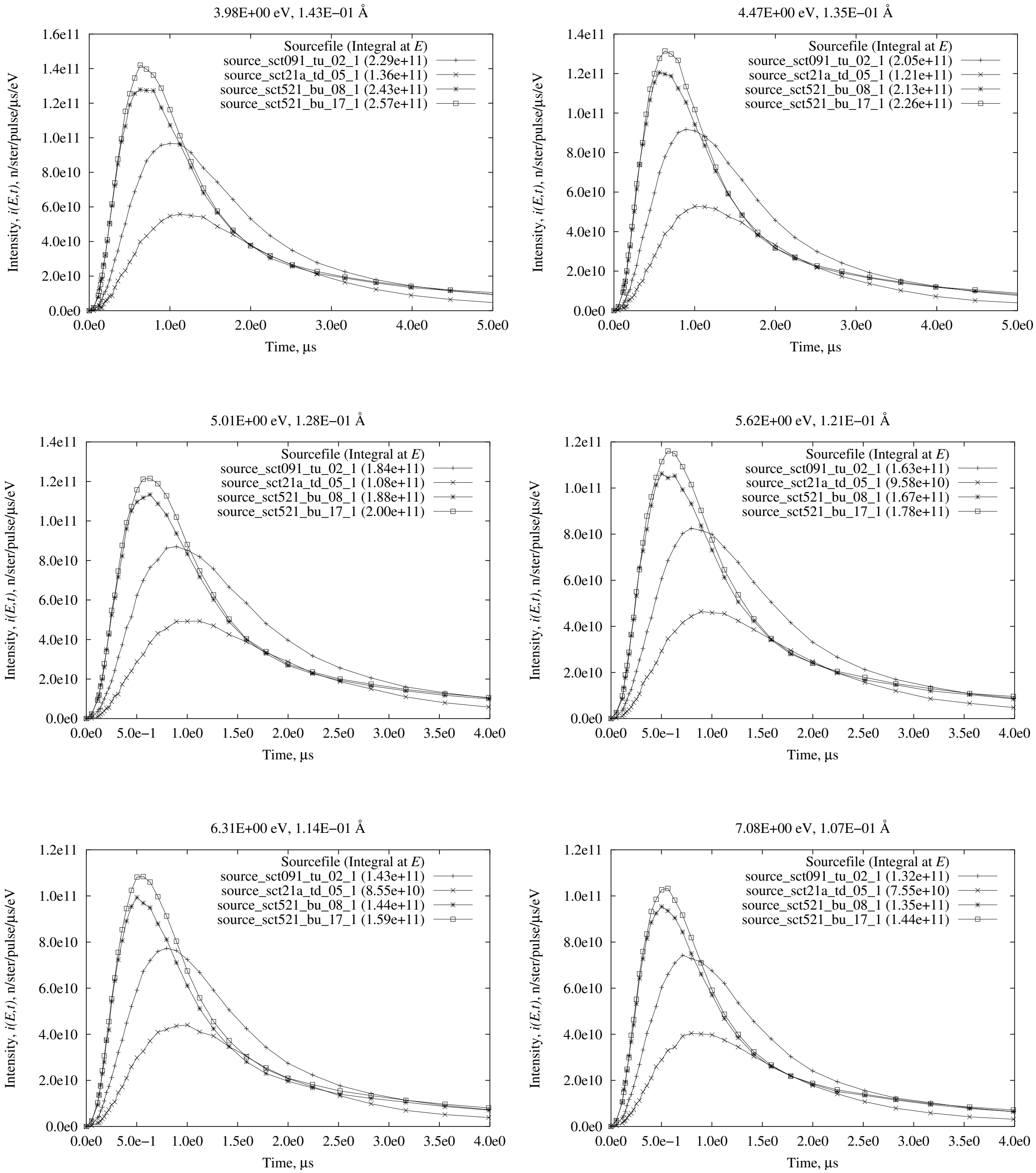

Figure 18: Emission time distributions. Results for 2TU (decoupled poisoned H_2) are denoted source_sct091_tu_02_1 and are similar to those for 11TU. Results for 5TD (coupled H_2) are denoted source_sct21a_td_05_1 and are similar to those for 14BD. Results for 8BU (decoupled H_2O poisoned at 15 mm) are denoted source_sct521_bu_08_1, and results for 17BU (decoupled H_2O poisoned at 25 mm) are denoted source_sct521_bu_17_1.

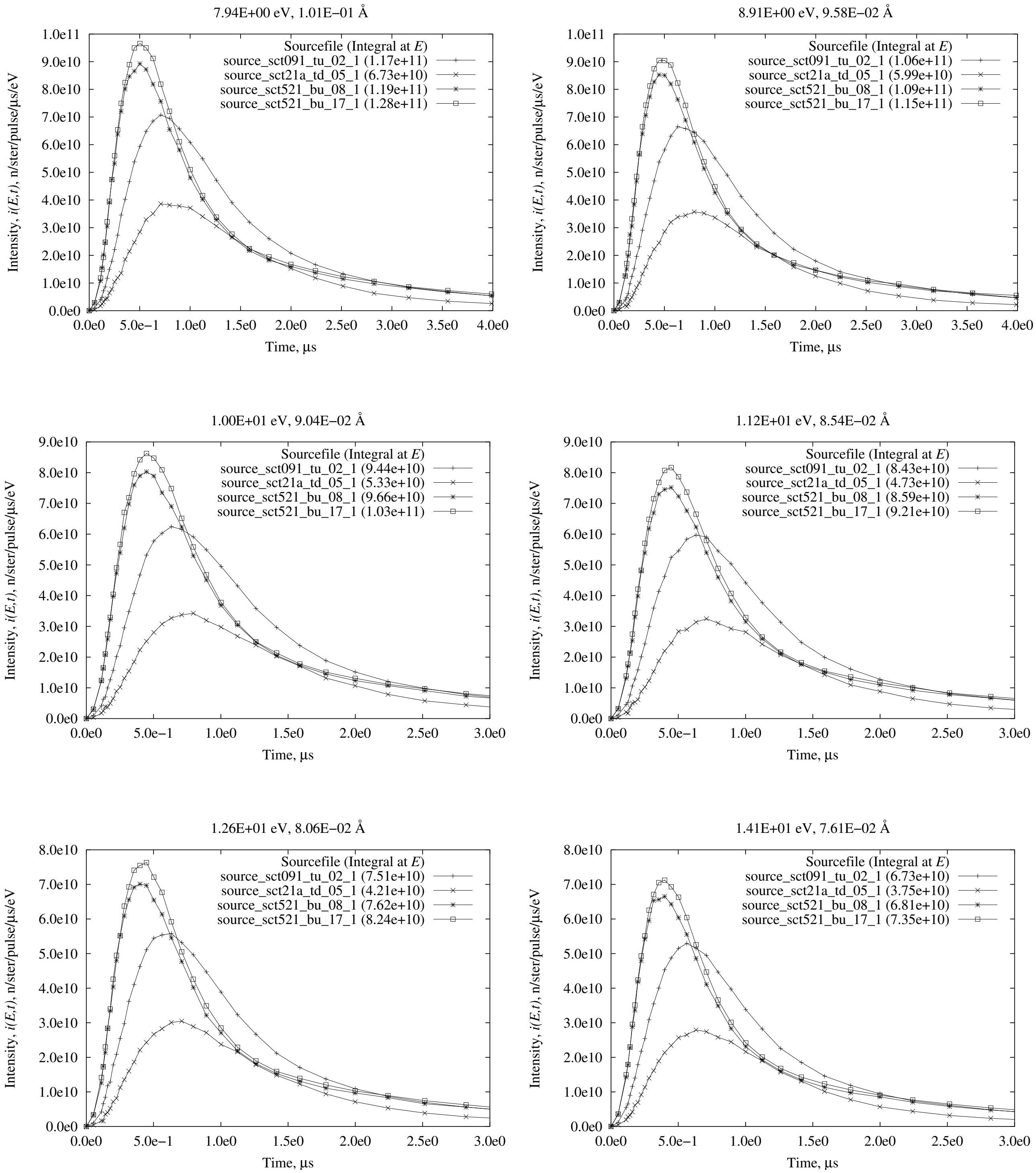

Figure 19: Emission time distributions. Results for 2TU (decoupled poisoned H_2) are denoted source_sct091_tu_02_1 and are similar to those for 11TU. Results for 5TD (coupled H_2) are denoted source_sct21a_td_05_1 and are similar to those for 14BD. Results for 8BU (decoupled H_2O poisoned at 15 mm) are denoted source_sct521_bu_08_1, and results for 17BU (decoupled H_2O poisoned at 25 mm) are denoted source_sct521_bu_17_1.